Optimization of Organic Electrochemical Transistors for Sensor Applications

Omid Yaghmazadeh,[1] Fabio Cicoira,[2] Daniel A. Bernards,[3] Sang Y. Yang,[4] Yvan Bonnassieux,[1] George G. Malliaras[5]

[1]Laboratory of Physics of Interfaces and Thin Films (LPICM), Ecole Polytechnique, Palaiseau 91120, France

[2]Institute of Photonics and Nanotechnology, CNR, Via alla Cascata 56/c, 38123 Povo (Trento), Italy

[3]Department of Bioengineering and Therapeutic Sciences, University of California, San Francisco, 1700 4th Street, San Francisco, California 94158-2330

[4]Department of Materials Science and Engineering, Cornell University, Ithaca, New York 14853-1501

[5]Centre Microélectronique de Provence, Ecole Nationale Supérieure des Mines de Saint Etienne, 880, route de Mimet, 13541 Gardanne, France

Correspondence to: G. G. Malliaras (E-mail: malliaras@emse.fr)

Received 29 July 2010; accepted 29 July 2010; published online 20 September 2010
DOI: 10.1002/polb.22129

ABSTRACT: Despite the recent interest in organic electrochemical transistors (OECTs) as chemical and biological sensors, little is known about the role that device architecture and materials parameters play in determining sensor performance. We use numerical modeling to establish design rules in two regimes of operation: We find that for operation as an ion-to-electron converter, the response of OECTs is maximized through the use of a gate electrode that is much larger than the channel or through the use of a nonpolarizable gate electrode. Improving the conductivity of the polymer and using a channel geometry that maximizes channel width and thickness, and minimizes channel length helps increase the response. For operation as an electrochemical sensor, the sensitivity is maximized in OECTs with gate electrodes that are smaller than their channels. The sensitivity can be improved by increasing the charge carrier mobility and the capacitance per unit area of the conducting polymer, and also its ability to be penetrated by ions from the electrolyte. A channel geometry that maximizes channel width and minimizes channel length also improves sensitivity. © 2010 Wiley Periodicals, Inc. J Polym Sci Part B: Polym Phys 49: 34–39, 2011

KEYWORDS: chemical and biological sensors; computer modeling; conjugated polymers; device modeling; organic electrochemical transistors; sensors

INTRODUCTION During the past two decades organic semiconductors have attracted a great deal of attention due to potential applications in a variety of low-cost electronic technologies.[1–3] A recent trend in the field involves the use of organic semiconductor devices in sensor applications.[4,5] Of particular interest in this arena are organic electrochemical transistors (OECTs, also known as conducting polymer transistors). First reported by Wrighton and coworkers[6] in the eighties, these devices are receiving renewed attention,[7–12] in particular as sensors for the detection of chemical and biological analytes. An OECT consists of a conducting polymer channel in contact with an electrolyte that has the gate electrode immersed in it (Fig. 1).

Poly(3,4-ethylenedioxythiophene) doped with poly(styrene sulfonate) (PEDOT:PSS), a degenerately doped *p*-type organic semiconductor, has emerged as the conducting polymer of choice in OECTs. This is because PEDOT:PSS is commercially available, can be processed into thin films from solution, yields films that are stable in a wide pH range, and has a high conductivity that allows the fabrication of not only the channel, but also the source, drain, and gate electrodes from the same material.[13,14] OECTs operate at low voltages, which makes them compatible with detection in aqueous environments. They can be miniaturized and integrated with microfluidic channels in a straightforward manner,[12,15] which makes them promising candidates for lab-on-a-chip applications. Finally, simple circuits can be built that condition the signal and improve sensitivity.[16]

OECTs have been used as *ion-to-electron converters*: The application of a positive gate voltage induces a transient ionic current in the electrolyte. Cations from the electrolyte enter the conducting polymer film and de-dope it (Fig. 1), thereby decreasing the drain current. Therefore, the OECT converts a transient ionic current into a change in the (electronic) drain current. Nilsson et al.[9] used this attribute to demonstrate an air humidity sensor. The device utilized Nafion—a proton conductor whose conductivity depends on humidity—as an electrolyte. Bernards et al.[10] used lipid

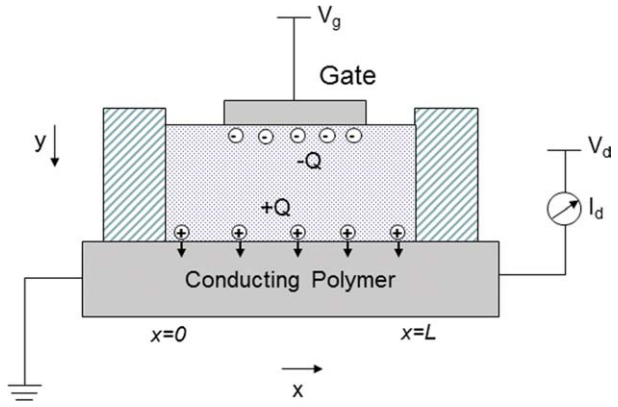

FIGURE 1 Schematic of a PDOT:PSS OECT indicating net charge distribution in the electrolyte after the application of a positive gate voltage.

bilayer membranes with gramicidin ion channels to selectively probe the transport of monovalent ions through the ion channels.

OECTs have also been used as *electrochemical sensors*: Charge transfer reactions between a species in the electrolyte and the gate electrode change the potential of the electrolyte, which results to a change in the drain current. Zhu et al.[8] used this fact to demonstrate a simple glucose sensor. They added the enzyme glucose oxidase (GOx) in the electrolyte of an OECT with a platinum gate electrode and showed that, in the presence of glucose, the drain current was dependent on the glucose concentration. The sensing mechanism was based on the fact that hydrogen peroxide, produced as a result of the GOx cycle, is oxidized at the gate electrode. This result was extended by Yang et al.[12] who used different redox enzymes to demonstrate that this concept can be generalized to yield multianalyte sensors. Cicoira et al.[17] fabricated planar OECTs with various ratios of channel to gate electrode area. They compared their ability to sense hydrogen peroxide and found that OECTs with smaller gates showed a higher sensitivity.

Although a great deal of progress has been made in understanding the mechanism of operation of OECTs,[11,18,19] comprehensive guidelines for their optimization in sensors are lacking. It is easy to imagine, for example, that different device architectures are optimal when using an OECT as an ion-to-electron converter or as an electrochemical sensor. Moreover, little is known about the role of materials parameters, such as conductivity of the polymer, play in determining sensor response. In this article, we use numerical modeling to explore the dependence of the relevant OECT characteristics on device geometry. We find that for operation as an ion-to-electron converter, the first design rule is to use a gate electrode that is much larger than the channel or to use a nonpolarizable gate electrode. The second design rule is to optimize the conductance of the channel, which necessitates the use of a geometry that maximizes channel width and minimizes channel length. For operation as an electrochemical sensor, OECTs with gate electrodes smaller than their channels show higher sensitivity. Their sensitivity can be increased by improving materials parameters of the conducting polymer such as its hole mobility and capacitance per unit area, and the ability of ions from the electrolyte to enter the polymer film. A geometry that maximizes channel width and minimizes channel length also can improve sensitivity.

OECTs AS ION-TO-ELECTRON CONVERTERS

A "thought" experiment in this regime would be as follows: A substance that is impermeable to ions and prevents the de-doping of the conducting polymer is placed on top of the transistor channel. Now let us assume that the permeability of this substance changes as a result of its interaction with an analyte, allowing access of ions from the electrolyte to the polymer. In this experiment, one would apply a gate voltage and look for changes in the drain current. The increased permeability of the barrier substance upon interaction with the analyte will be revealed by a modulation of the drain current, induced by the application of the gate voltage. In this experiment one would seek to maximize the change of the drain current (I_d) upon the application of a gate voltage (V_g), hence the response of the transducer is related to the transconductance $\partial I_d/\partial V_g$.

To understand how $\partial I_d/\partial V_g$ varies with device geometry, we conducted numerical simulations according to Bernards et al.,[11,19] as outlined in the experimental part. The transfer characteristics of three OECTs with $A_{ch}/A_g = 0.01$, 1, and 100 (where A_{ch} is the area of the channel and A_g is the area of the gate electrode) are shown in Figure 2. The transistor with the small gate ($A_{ch}/A_g = 100$) shows little modulation of the drain current and it stays in the ON state throughout the range of gate applied bias. On the contrary, the transistor with the large gate ($A_{ch}/A_g = 0.01$) shows the highest modulation of the drain current, hence, the highest value of $\partial I_d/\partial V_g$, and therefore would be the most suitable to use as an ion-to-electron converter.

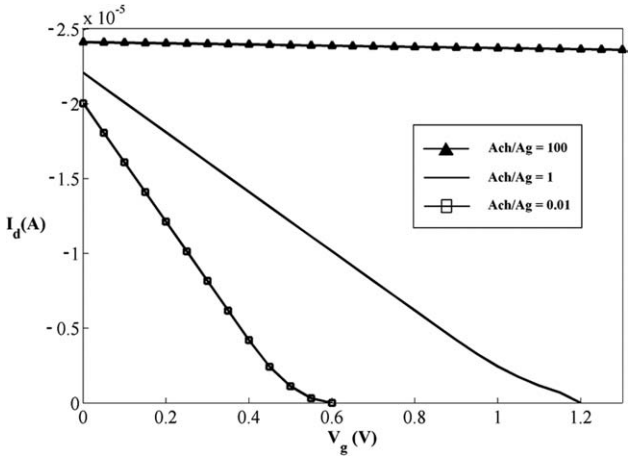

FIGURE 2 Simulated transfer characteristics of OECTs for three different device geometries ($A_{ch}/A_g = 0.01$, 1, and 100) and for $V_d = -0.2$V.

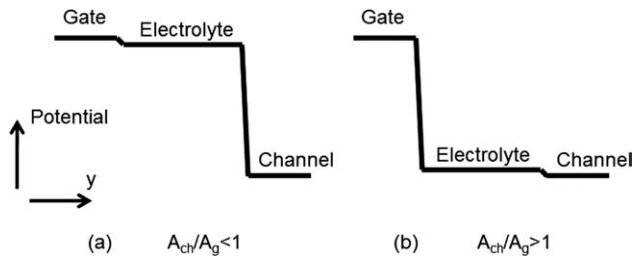

FIGURE 3 Potential distribution between the gate electrode and the channel for two device geometries.

The data of Figure 2 can be understood by considering the potential distribution between the gate and the channel. Two extreme cases are shown in Figure 3(a,b) (we assumed that the channel is at zero potential, which holds for $V_d \ll V_g$). The electrolyte potential V_{sol} in this case is determined by the capacitances associated with double layer formation at the gate and the channel and is equal to:[11]

$$V_{sol} = \frac{V_g}{1 + \frac{c_{ch} \cdot A_{ch}}{c_g \cdot A_g}}, \quad (1)$$

where c_{ch} and c_g are the channel and gate capacitance per unit area, respectively. It should be noted that eq 1 holds when both the gate electrode and the conducting polymer channel are polarizable. This is a good approximation for metals such as Pt, but ions do penetrate polymers such as PEDOT:PSS and de-dope them. Therefore, the capacitance associated with the polymer channel in eq 1 should be viewed as an effective quantity that is mechanistically distinct than double layer formation at a polarizable metal electrode.[20] In our model, we assumed $c_{ch} = c_g$ to focus on the influence of device geometry. The reader should keep in mind that it is the product of $c \times A$ that matters, hence the OECT response can also be tuned via appropriate selection of materials. Finally, it should be noted that if a nonpolarizable electrode such as Ag/AgCl is used as the gate, then there will be no potential drop at the gate/electrolyte interface. The potential distribution in this case will be closer to that of Figure 3(a), regardless of the area of the gate electrode.

According to the above, in the transistor with the large gate electrode, the electrolyte is nearly at the same potential as the gate. This results into a large potential drop between the electrolyte and the channel [Fig. 3(a)], which, in turn, leads to a strong modulation of the drain current. On the contrary, in the transistor with the small gate electrode, the applied potential drops at the gate/electrolyte interface [Fig. 3(b)] and the resulting modulation of the drain current is weak. Therefore, for operation as an ion-to-electron converter, the first design rule is to use a gate electrode that is much larger than the channel. An alternative would be to use a nonpolarizable gate electrode.

It should be noted that the potential distribution within the OECT has a large influence on the output characteristics of the transistor. Figure 4(a,b) shows the output characteristics of two OECTs made with PEDOT:PSS channels and gates, with $A_{ch}/A_g = 0.1$ and 10, respectively. The output characteristics of the transistor with the large gate [Fig. 4(a)] show a large modulation of the drain current, while the modulation of the drain current is small in the transistor with the small gate [Fig. 4(b)]. For the case of interest here (large gate, hence $V_{sol} \approx V_g$), the drain current is in the saturation regime under regular operation conditions, and can be expressed as:[19]

$$I_d = -G \cdot \frac{(V_g - V_p)^2}{2 \cdot V_p}, \quad (2)$$

where G is the conductance of the channel, and V_p the pinch-off voltage. The latter is a measure of the dopant density in the conducting polymer relative to the ionic charge supplied from the electrolyte, and indicates the onset of saturation in the absence of a gate bias. From this equation it can be shown that for an OECT with a large gate electrode:

$$\left.\frac{\partial I_d}{\partial V_g}\right|_{V_g=0} = -G. \quad (3)$$

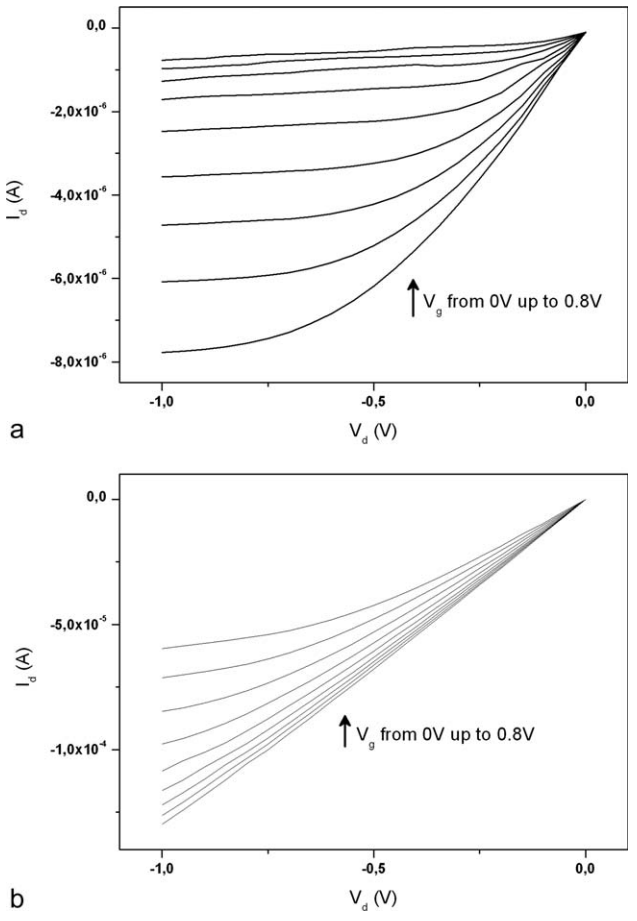

FIGURE 4 Output characteristics of planar PEDOT:PSS OECTs with $A_{ch}/A_g = 0.1$ (a) and $A_{ch}/A_g = 10$ (b).

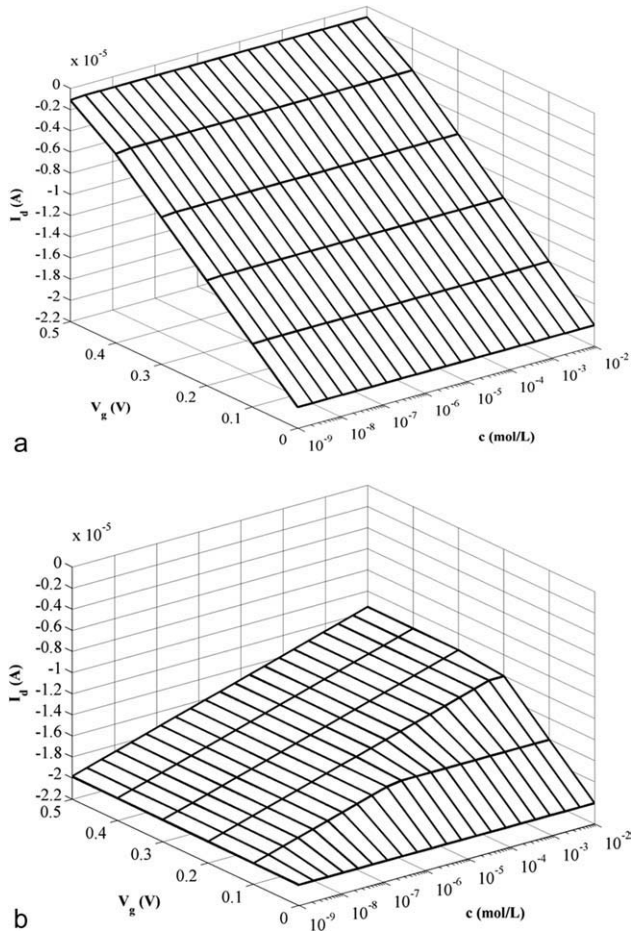

FIGURE 5 Simulated response of OECTs to an analyte, for two different device geometries, (a) $A_{ch}/A_g = 0.01$, and (b) $A_{ch}/A_g = 100$, and for $V_d = -0.2$ V.

The above equation shows that the response of an OECT with a large gate depends on the conductance of the channel, which is the product of the conductivity of the polymer and the geometrical factor $W\,d/L$ (W and L are the channel width and length, respectively, and d the thickness of the polymer film). This is the second design rule and it calls for the use of a conducting polymer with as high conductivity as possible, but also with a channel geometry that maximizes channel width and thickness, and minimizes channel length.

OECTs AS ELECTROCHEMICAL SENSORS

In this regime, the gate electrode, which is used as the working electrode, is held at a constant voltage. Charge transfer between an analyte (or a mediator, whose concentration relates to the analyte one wishes to detect) and the gate electrode raises the potential of the electrolyte by a value $V_{analyte}$ described by the Nernst equation:

$$V_{analyte} = \frac{k \cdot T}{2 \cdot e} \cdot \ln[C] + \text{const.}, \qquad (4)$$

where k is the Boltzmann constant, T is the absolute temperature, e is the fundamental charge, C is the concentration of the analyte, and the constant contains details such as the formal potential. Therefore, the addition of analyte results to a decrease in the potential drop at the gate electrode/electrolyte interface, and a concomitant increase in the potential drop at the electrolyte/channel interface (since the gate is held at a constant voltage). As a result, the drain current responds to this change in a way that relates to the analyte concentration.[11]

Figure 5 shows the results of computer modeling of I_d for two OECTs with $A_{ch}/A_g = 0.01$ and 100, to various concentrations of analyte and to different gate voltages. The results show that in the OECT with the large gate [Fig. 5(a)] the drain current does not change with analyte concentration, even when the later is varied by several orders of magnitude. On the contrary, in the OECT with the small gate, the drain current responds well to the analyte [Fig. 5(b)], especially at higher gate voltages. A key sensor parameter is the sensitivity, defined as the slope of the I_d versus C curve. Figure 6 shows the sensitivity (calculated for $V_g = 0.5$ V and $V_d = -0.2$ V, and normalized to 1) as a function of A_{ch}/A_g. The data shows that OECTs with small gates show higher sensitivity than OECTs with large gates, in agreement with the findings of Cicoira et al.[17] The sensitivity saturates at both limits of A_{ch}/A_g, to zero for OECTs with large gates and to a maximum value for OECTs with small gates, respectively. Therefore, for operation as an electrochemical sensor, the first design rule is to use a gate electrode that is smaller than the channel.

The data of Figure 6 can be understood by considering the potential diagrams of Figure 2. The reason for the zero sensitivity in OECTs with large gates lies in the fact that the potential drop at the gate electrode/electrolyte interface becomes infinitesimally small, and does not change appreciably when the analyte is added. A similar argument explains the saturation of sensitivity for OECTs with small gates: When the potential drop at the gate electrode/electrolyte interface becomes comparable to the applied gate voltage, the device achieves its maximum sensitivity. The value of A_{ch}/A_g for which this occurs depends on several parameters, including the drain voltage and the ratio of capacitance per unit area of

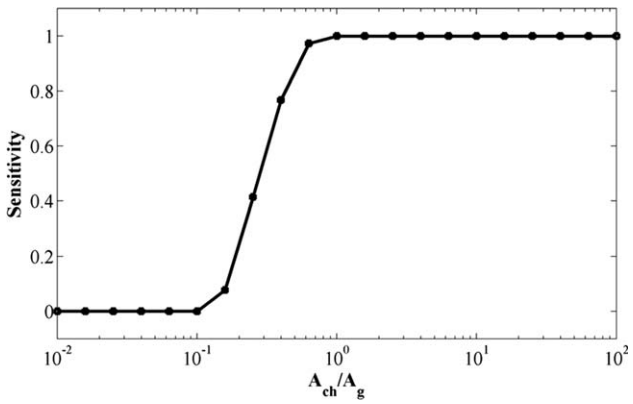

FIGURE 6 Simulated sensitivity of OECT-based enzymatic sensors as a function of device geometry, calculated for $V_g = 0.5$ V and $V_d = -0.2$ V, and normalized to 1.

gate electrode and channel. For a larger drain voltage, the sensitivity transition from zero to one occurs over a narrower region of A_{ch}/A_g values. For a larger capacitance per unit area of the channel (compared to that of the gate electrode), the whole curve shifts towards lower A_{ch}/A_g values.

For OECTs with small gates, the drain current is in the linear regime (see Fig. 4) under regular operating conditions, and can be expressed as:[19]

$$I_d = -G \cdot \left(1 - \frac{V_{sol}}{V_p} + \frac{V_d}{2 \cdot V_p}\right) \cdot V_d. \quad (5)$$

From eqs 4 and 5 we obtain the sensitivity:

$$\frac{\partial I_d}{\partial C} = G \cdot \frac{k \cdot T}{2 \cdot e} \cdot \frac{V_d}{V_p} \cdot \frac{1}{C} = \frac{k \cdot T}{2 \cdot e} \cdot \frac{1}{C} \cdot \mu \cdot \frac{W}{L} \cdot \beta \cdot c_{ch} \cdot V_d, \quad (6)$$

where μ is the hole mobility in the channel, β is the fraction of ions at the electrolyte/channel interface that penetrate into the channel (see experimental section). For the derivation above we used the fact that the pinch-off voltage is equal to $e \times p_0 \times d/(\beta \times c_{ch})$, where p_0 is the hole density in the conducting polymer. Equation 6 shows that the response of an OECT with a small gate depends on the hole mobility in the conducting polymer, its ability to uptake ions from the solution, and its capacitance per unit area. This is the second design rule and it defines materials parameters to be optimized, but also calls for a channel geometry that maximizes channel width and minimizes channel length. It should be noted that eq 6 shows that the sensitivity is inversely proportional to analyte concentration: This is due to the fact that the drain current is proportional to the logarithm of the analyte concentration.

CONCLUSIONS

In conclusion, we used numerical modeling to derive guidelines for optimization of OECT geometry for sensor applications. For operation as an ion-to-electron converter, a gate electrode that is much larger than the channel, or one that is made from a nonpolarizable gate electrode is recommended. A channel with a high conductance is also recommended. For operation as an electrochemical sensor, we find that an OECT with a gate electrode that is smaller than the channel shows higher sensitivity. The response can be increased by improving the hole mobility and capacitance per unit area of the conducting polymer, and the ability of ions from the electrolyte to enter the polymer film. A geometry that maximizes channel width and minimizes channel length is recommended in both cases.

EXPERIMENTAL

Modeling

We followed the model introduced by Bernards et al.[11,19] and used the same input parameters. Two previous simplifications were relaxed to improve accuracy:

The first modification accounts explicitly for the variation of the potential over the surface of the channel. Since the voltage at the channel surface depends on position x, one can interpret the stored charge as a sum of smaller charges stored on sliced channel surfaces, each of dx length given by:

$$Q = \sum_i c_{ch} \cdot dx \cdot W \cdot (V_{sol} - V(x)), \quad (7)$$

where c_{ch} is the capacitance per unit area at the electrolyte/channel interface and W is the channel width. If one takes dx small enough, then the sum can be approximated by:

$$Q = c_{ch} \cdot A_{ch} \cdot V_{sol} - c_{ch} \cdot W \cdot \int_{x=0}^{L} V(x) \cdot dx. \quad (8)$$

Here L is the channel length and A_{ch} represents the channel area and is equal to the product of channel width W and length L. Considering that the total electrolyte-channel capacitance C_{ch} is equal to $c_{ch} \times A_{ch}$, the electrolyte potential becomes:

$$V_{sol} = V_g \cdot \frac{C_g}{C_{ch} + C_g} + \frac{c_{ch} \cdot W}{C_{ch} + C_g} \cdot \int_{x=0}^{L} V(x) \cdot dx. \quad (9)$$

The second modification treats the issue of polarizability of the polymer channel more explicitly. As discussed above, polymers in the general case lie between the two limits of polarizable and nonpolarizable electrode. We therefore introduced a new parameter β (and fixed its value to 0.5 for this work) which is defined as the fraction of ions at the electrolyte/channel interface that penetrate into the channel. Therefore, $\beta = 0$ corresponds to a perfectly polarizable interface while $\beta = 1$ corresponds to a perfectly nonpolarizable interface. Consequently, the charge transferred from the electrolyte into the polymer, for a position x through the channel, can be expressed using a gradual charge approximation, and is given by:

$$Q_i(x) = c_{ch} \cdot dx \cdot W \cdot \beta \cdot (V_{sol} - V(x)). \quad (10)$$

Fabrication

For the fabrication of the OECTs, PEDOT:PSS was patterned using an additive lift-off process described in literature.[21] A parylene film was deposited on a microscope objective and patterned by conventional photolithography and oxygen plasma etching. A PEDOT:PSS mixture (Clevios PH500, HC Starck)/ ethylene glycol (4:1 by volume) was spin-coated on the patterned parylene layer and baked at 140 °C for 1 h before the parylene film was mechanically peeled-off, creating the desired PEDOT:PSS pattern. It is worth noting that 0.5 wt % of 3-glycidoxypropyltrimethoxysilane was added to PEDOT:PSS mixture to improve the stability of PEDOT:PSS film in aqueous solution by increasing the adhesion strength between PEDOT:PSS film and glass substrate. The resulting device was composed of a pair of 0.1 mm-wide and 1 mm-wide PEDOT:PSS stripes. To complete OECT testing structure, a PDMS well that contained the electrolyte solution was placed over a pair of PEDOT:PSS stripes. Phosphate buffer saline (PBS, pH ~ 7) was used as the electrolyte.

REFERENCES AND NOTES

1 Malliaras, G.; Friend, R. *Phys. Today* **2005**, *58*, 53–58.

2 Lin, F. D.; Lonergan, M. C. *Appl. Phys. Lett.* **2006**, *88*, 133507.

3 Hsu, F. C.; Prigodin, V. N.; Epstein, A. J. *Phys. Rev. B* **2006**, *74*, 235219.

4 Berggren, M.; Richter-Dahlfors, A. *Adv. Mater.* **2007**, *19*, 3201–3213.

5 Organic Semiconductors in Sensor Applications, Bernards, D.; Owens, R. M.; Malliaras, G. G., Eds.; Springer: Berlin Heidelberg, **2008.**

6 White, H. S.; Kittlesen, G. P.; Wrighton, M. S. *J. Am. Chem. Soc.* **1984**, *106*, 5375.

7 Mabeck, J. T.; Malliaras, G. G. *Anal. Bioanal. Chem.* **2006**, *384*, 343–353.

8 Zhu, Z. T.; Mabeck, J. T.; Zhu, C. C.; Cady, N. C.; Batt, C. A.; Malliaras, G. G. *Chem. Commun.* **2004**, 1556–1557.

9 Nilsson, D.; Kugler, T.; Svensson, P. O.; Berggren, M. *Sens. Actuators B-Chem.* **2002**, *86*, 193.

10 Bernards, D. A.; Malliaras, G. G.; Toombes, G. E. S.; Gruner, S. M. *Appl. Phys. Lett.* **2006**, *89*, 053505.

11 Bernards, D. A.; Macaya, D. J.; Nikolou, M.; DeFranco, J. A.; Takamatsu, S.; Malliaras, G. G. *J. Mater. Chem.* **2008**, *18*, 116–120.

12 Yang, S. Y.; DeFranco, J. A.; Sylvester, Y. A.; Gobert, T. J.; Macaya, D. J.; Owens, R. M.; Malliaras, G. G. *Lab on a Chip* **2009**, *9*, 704–708.

13 Andersson, P.; Nilsson, D.; Svensson, P. O.; Chen, M. X.; Malmstrom, A.; Remonen, T.; Kugler, T.; Berggren, M. *Adv. Mater.* **2002**, *14*, 1460–1464.

14 Shim, N. Y.; Bernards, D. A.; Macaya, D. J.; DeFranco, J. A.; Nikolou, M.; Owens, R. M.; Malliaras, G. G. *Sensors-Basel.* **2009**, *9*, 9894–9902.

15 Mabeck, J. T.; DeFranco, J. A.; Bernards, D. A.; Malliaras, G. G.; Hocde, S.; Chase, C. J. *Appl. Phys. Lett.* **2005**, *87*, 1–3.

16 Svensson, P. O.; Nilsson, D.; Forchheimer, R.; Berggren, M. *Appl. Phys. Lett.* **2008**, *93*, 203301.

17 Cicoira, F.; Sessolo, M.; Yaghmazadeh, O.; DeFranco, J. A.; Yang, S. Y.; Malliaras, G. G. *Adv. Mater.* **2010**, *22*, 1012–1016.

18 Robinson, N. D.; Svensson, P.-O.; Nilsson, D.; Berggren, M. *J. Electrochem. Soc.* **2006**, *153*, H39–H44.

19 Bernards, D. A.; Malliaras, G. G. *Adv. Funct. Mater.* **2007**, *17*, 3538–3544.

20 Wang, J.; Bard, A. J. *J. Am. Chem. Soc.* **2001**, *123*, 498–499.

21 DeFranco, J. A.; Schmidt, B. S.; Lipson, M.; Malliaras, G. G. *Org. Electron.* **2006**, *7*, 22–28.